Correspondence

Automatic Target Recognition of Military Vehicles With Krawtchouk Moments

The challenge of automatic target recognition of military targets within a synthetic aperture radar scene is addressed in this paper. The proposed approach exploits the discrete-defined Krawtchouk moments, which are able to represent a detected extended target with few features, allowing its characterization. The proposed algorithm provides robust performance for target recognition, identification, and characterization, with high reliability in the presence of noise and reduced sensitivity to discretization errors. The effectiveness of the proposed approach is demonstrated using the MSTAR dataset.

I. INTRODUCTION

Target recognition of military vehicles is a topic of increasing interest and demanding requirements [1], [2]. The knowledge of the vehicles deployed in a specific area of interest is fundamental to the understanding of the threat that exists (e.g., small intercontinental ballistic missile launcher rather than a theater missile launcher). Furthermore, it also allows a better understanding of the activities in a specific site. Currently, there is a growing interest in the ability to increase the level of knowledge to the identification or characterization stage, where the actual capabilities of the vehicle/object can be better understood. Many current automatic target recognition (ATR) algorithms for vehicles require the ability to identify small differences among targets like a specific configuration of a multirole vehicle. Furthermore, ATR represents one of the multiple tasks in which modern platforms are involved. For example, an unmanned aerial vehicle (UAV) will be acquiring the radar echoes, performing the imaging using high-performance computing capabilities [3], maintaining constant communication with a control center or other platforms, while managing other systems like electro-optical sensors. For this reason, the processing and the information extraction have to comply with the low Size Weight And Power (SWAP) paradigm.

Various approaches have been proposed to address the ATR challenge. A general approach has been investigated in [4], where L_2 normalization is applied to the image,

Manuscript received November 5, 2015; revised April 29, 2016; released for publication July 30, 2016. Date of publication January 17, 2017; date of current version April 17, 2017.

DOI. No. 10.1109/TAES.2017.2649160

Refereeing of this contribution was handled by S. Watts.

This work was supported by the Engineering and Physical Sciences Research Council under Grant EP/K014307/1 and the MOD University Defence Research Collaboration in Signal Processing and the University of Naples "Federico II".

thereby preserving all the information of the image while assigning to the classifier the task of deriving the model and separation of targets. After L_2 normalization, the synthetic aperture radar (SAR) chips containing the target are passed to the support vector machine (SVM) that uses a Gaussian kernel, with the kernel size set to be the average Euclidean distance between training patterns. The SVM approach was tested on the MSTAR dataset and compared with other classifiers such as model matching and neural network. The work developed at the MIT Lincoln Laboratory [1] provides a complete analysis by investigating both detection and classification of stationary ground targets using high-resolution fully polarimetric SAR images. The algorithm comprises three main stages: detection (or prescreening), discrimination, and classification. In particular, a mean-square-error (MSE) classifier is exploited in this algorithm, whose minimum acceptable value is thresholded, and targets that differ more than the threshold from the target model are labeled as clutter. The main drawback of the algorithm is the fact that it relies on a single metric (MSE), meaning that an accurate knowledge of the target models is required; otherwise, the algorithm would incur in misclassification. A robust algorithm has been proposed in [5], in which an increased number of scattering centres are selected while retaining low computational complexity. The approach uses a relatively large number of scatterers with a variability reduction technique. To reduce the effect of the variabilities, a novel grid cell structure is developed by considering the information of potential targets, such as target sizes, structures, and relative positions of the strongest scatterers. Furthermore, features related to scatterer angular stability information are extracted. Discriminative graphical models have been used in [6] with the aim to fuse different features and allow good performance with small training datasets. A two-stage framework is proposed to model dependencies between different feature representations of a target image. The approach has been tested using the MSTAR dataset and the performance resulted to overcome EMACH, SVM, AdaBoost, and Conditonal Gaussian Model classifiers.

In this paper, an algorithm for ATR based on the Krawtchouk moments is proposed. The characterization capability and reliability of the new method are investigated. The Krawtchouk moments were introduced in [7] and [8] for image-processing application purposes. The Krawtchouk moments have been applied to 1-, 2-, and 3-D signals [9]–[12]. In [9], a method using the Krawtchouk moments was proposed to enhance noise-corrupted speech signals. In particular, Wiener filtering was applied after representing a noisy signal in the Krawtchouk and Tchebychev domains. Image super-resolution was proposed in [10] for the specific case of low-resolution video sequences. The authors of [10] used Krawchouk moments to create a high-resolution image sequence from a given low-resolution image sequence, as they are orthogonal over a square region, and are discrete moments. A Krawtchouk-based noise resilient gait recognition from videos was proposed in [11]. In this approach, the orthogonality of the moments was exploited in order to ensure minimal redundancy. Finally, the extension to 3-D of the Krawtchouk polynomials was used for shape search and retrieval in [12]. In particular, the property of the low-order Krawtchouk moments to capture edges was exploited in order to obtain enhanced discrimination of 3-D objects with low complexity.

A common issue of most of the families of image moments [13] is the level of discretization error and poor robustness in low-signal-to-noise-ratio (SNR) conditions. This error builds up as the order increases, limiting the accuracy of the computed moments. This drawback results in target recognition algorithms with less accuracy in discriminating between targets that differ in small components, which would be possible if only robust higher order moments are used.

The Krawtchouk moments have some peculiar characteristics [8], in particular they are discretely defined; thus, there is no requirement of spatial normalization, and the discretization error is nonexistent. This translates in a relaxation on the amount of resources required to represent and store the polynomials. Moreover, the computational cost is reduced due to the orthogonality property of the Krawtchouk polynomials that relaxes the requirements of feature selection to mitigate overfitting. These characteristics, together with the capability to precompute the polynomials, make this family of image moments compatible with SWAP systems.

The remainder of this paper is organized as follows. Section II introduces the Krawthcouk moments and describes the proposed ATR algorithm. Section III discusses the results obtained using the MSTAR dataset in different noise conditions. Section IV concludes this paper.

II. ATR ALGORITHM BASED ON THE KRAWTCHOUK MOMENTS

This section describes the ATR algorithm that is based on the Krawtchouk moments. First, the analytical formulation of the Krawtchouk moments is provided in order to support the understanding of the algorithm functional blocks described successively in detail.

A. Krawtchouk Moments

The classical formulation of the Krawtchouk polynomials introduced in [7] suffers from numerical instability. For this reason, the weighted Krawtchouk polynomials that were introduced in [8] have been selected for the purpose of representing the target in the proposed ATR approach.

The classical Krawtchouk polynomials of order n are defined as [8]

$$K_n(x; p, N) = \sum_{k=0}^{N} a_{k,n,p} x^k = {}_2F_1\left(-n, -x; -N; \frac{1}{p}\right) \tag{1}$$

where x and n belong to $(0, 1, 2, \ldots, N)$, $N \in \mathbb{N}$, where $\mathbb{N}$ is the set of natural numbers, p is a real number belonging to

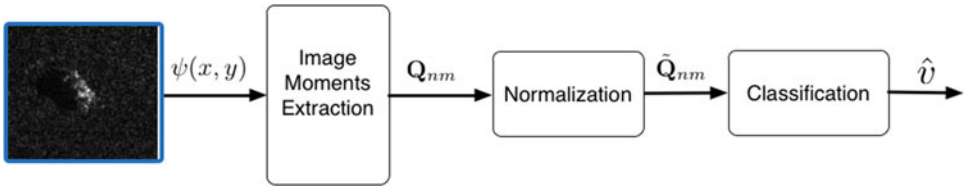

Fig. 1. Block diagram of the proposed feature extraction and classification algorithm.

the set (0, 1), and ${}_2F_1$ is the Gauss hypergeometric function

$$ {}_2F_1(a, b; c; z) = \sum_{k=0}^{\infty} \frac{(a)_k (b)_k}{(c)_k} \frac{z^k}{k!} \tag{2} $$

where $(\cdot)_k$ is the Pochhammer symbol given by

$$ (a)_k = a(a+1)\dots(a+k-1) = \frac{\Gamma(a+k)}{\Gamma(a)} \tag{3} $$

and $\Gamma(\cdot)$ is the Eulerian Gamma function.

To overcome the numerical instability of these polynomials, a weight [8] can be used leading to the weighted Krawtchouk Polynomials, i.e.,

$$ \bar{K}_n(x; p, N) = K_n(x; p, N) \sqrt{\frac{w(x; p, N)}{\rho(n; p, N)}} \tag{4} $$

with $w(x; p, N) = \binom{N}{x} p^x (1-p)^{N-x}$ and $\rho(n; p, N) = (-1)^n \left(\frac{1-p}{p}\right)^n \frac{n!}{(-N)_n}$.

The polynomials defined in (4) are orthogonal, i.e.,

$$ \sum_{x=0}^{N} \bar{K}_n(x; p, N) \bar{K}_m(x; p, N) = \delta_{nm} \quad \forall p, N \tag{5} $$

where $\delta_{nm} = 1$ if $n = m$, 0 otherwise, with $(n, m) \in (0, 1, \dots, N)^2$. Furthermore, the parameter p represents a shift parameter. In particular, as p deviates from the value 0.5 by Δp, the weighted Krawtchouk polynomials are approximately shifted by $N\Delta p$ [8]. This characteristic can be exploited to focus on a specific area of interest within the image, for example, by increasing the number of features related to a specific section of a target (e.g., a tank turret) in order to improve the target characterization capabilities. Considering a 2-D function of interest $\psi(x, y)$, e.g., a SAR image, with x and y natural numbers in the sets $(1, N)$ and $(1, M)$, respectively, and M and N representing the image width and height in samples, the Krawtchouk moments of order (n, m) are defined as

$$ Q_{nm} = \sum_{x=0}^{N-1} \sum_{y=0}^{M-1} \bar{K}_n(y; p_1, N-1) \bar{K}_m(x; p_2, M-1) \psi(x, y). \tag{6} $$

The moments in (6) provide a powerful tool for representing 2-D functions with a limited set of values and have been previously used for image compression and recognition [14].

B. Algorithm Description

The functional blocks of the proposed ATR algorithm are depicted in Fig. 1. The starting point is the intensity SAR image, $\psi(x, y)$, of a target from the set of J possible targets of interest. Equation (6) can be applied to $\psi(x, y)$ for each order up to (n, m) to form the vector $\mathbf{Q}_{nm}$ containing the Krawtchouk moments

$$ \mathbf{Q}_{nm} = [Q_{00}, \dots, Q_{nm}]. \tag{7} $$

From (6), it is also possible to estimate the computational complexity of the proposed approach for feature extraction that results to be equal to $(N \times M)^2$. The feature vector $\mathbf{Q}_{nm}$ has $(n+1) \times (m+1)$ elements and is normalized using the following standardization to ensure that any particular feature will not have a higher impact on the classification stage [15]:

$$ \tilde{\mathbf{Q}}_{nm} = (\mathbf{Q}_{nm} - \mu_{\mathbf{Q}_{nm}}) / \sigma_{\mathbf{Q}_{nm}} \tag{8} $$

where $\mu_{\mathbf{Q}_{nm}}$ and $\sigma_{\mathbf{Q}_{nm}}$ are, respectively, mean and standard deviation of $\mathbf{Q}_{nm}$.

The feature vectors are then used as input to a classification algorithm, such as k-nearest neighbors (k-NN), SVM, or Bayesian classifier. The output of the classifier is $\hat{v}$, with values in $(1, J) \in \mathbb{N}$ containing the output target class identifier of the image under test.

III. PERFORMANCE ANALYSIS ON THE MSTAR DATASET

In this section, the performance analysis of the proposed algorithm is assessed on real data. The MSTAR dataset is a collection of SAR images of 14 different military targets [16], [17], which represents a useful test bench for ATR algorithms. This dataset can be used for the different levels of target classification. According to the NATO AAP-6 Glossary Terms and Definitions, with "recognition" is meant the classification of the type/category of target; "identification" regards the capability to assign the target to a subclass; "characterization" takes into account the class variants. Following this definition, Table I reports the different targets and their grouping in the MSTAR dataset, together with the number of available images acquired with 15° and 17° of depression angle.

The images are supposed to cover the full 360° azimuth angle. However, due to missing images in the dataset, the total number of observations does not always cover each aspect angle. Moreover, different targets have different

TABLE I
MSTAR Dataset

Target	Type	# of Images 15–17°	Recognition	Identification	Characterization
BMP2 9563	Tank	195–233	R1	I1	C1
BMP2 9566	Tank	196–232			C2
BMP2 C21	Tank	196–233			C3
T72 132	Tank	196–232		I2	C4
T72 812	Tank	195–231			C5
T72 S7	Tank	191–228			C6
2S1	Tank	276–299		I3	C7
T62	Tank	273–299		I4	C8
ZSU	Tank	274–299		I5	C9
BTR70 C71	Personnel Carrier	196–233	R2	I6	C10
BTR60	Personnel Carrier	195–256		I7	C11
ZIL131	Truck	274–299	R3	I8	C12
BRDM	Reconn. Vehicle	274–298	R4	I9	C13
D7	Bulldozer	274–299	R5	I10	C14

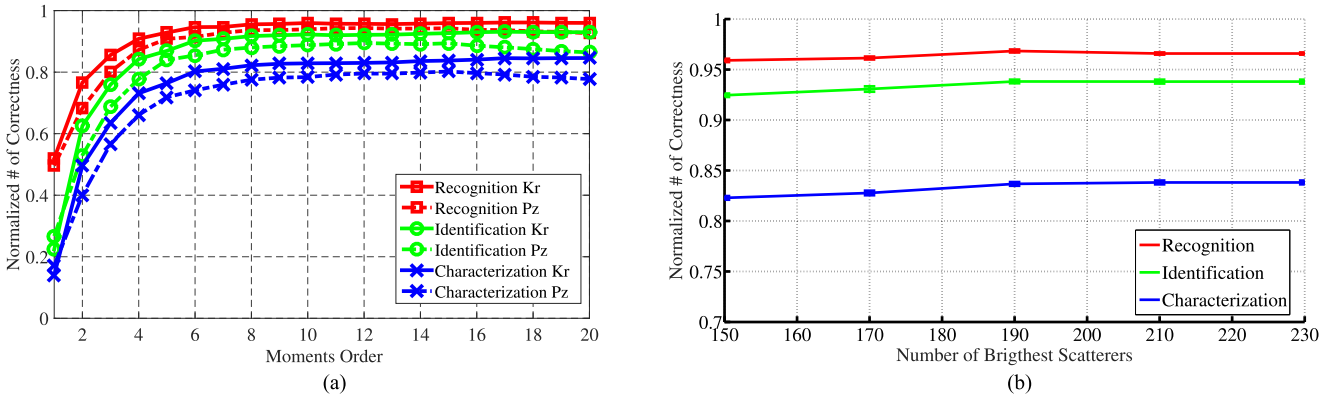

Fig. 2. Performance in terms of normalized correct number of recognition, identification, and characterization on the MSTAR dataset for (a) the proposed algorithm using the Krawtchouk moments versus the algorithm introduced in [18] using the pseudo-Zernike moments and (b) compared with the performance achievable using the approach in [5] for various number of brightest scatterers selected.

number of images. In the performance analysis, 191 samples are used as the minimal number of images available for all the targets. The training images are selected randomly, and the same number of images for each target from the set of images acquired at 15° of depression angle is considered. In order to investigate the robustness of the algorithm for different training sets available, the selection of the images used for testing and those used for training is randomized in each run. In this way, a different subset of training images is drawn, and, consequently, a different subset of test images is used in the testing stage. Specifically, a total of 100 Monte Carlo runs are performed for each analysis in order to be able to draw randomly a wider set of training and test images for the targets with more than 191 images available.

In order to investigate the capabilities and the robustness of the proposed approach, the results of the new algorithm are compared to those obtained using the pseudo-Zernike moments [18] and the approach proposed in [5]. In the experiments, a k-NN classifier with $k = 3$ and $p_1 = p_2 = 0.5$ for the computation of the Krawtchouk polynomials have been used. Fig. 2(a) shows the normalized average number of correct recognition, identification, and characterization obtained for both Krawtchouk and pseudo-Zernike approaches. In the analysis, all the moments available up to a selected order are considered.

It is seen that the Krawtchouk-based algorithm is superior to the pseudo-Zernike-based algorithm for all the three levels of target discrimination. For example, considering moments of order up to 20 (441 features), the percentage of correct target recognition reaches 96.02% using the proposed algorithm, while it is 92.64% for the pseudo-Zernike algorithm. A similar trend is seen for the target identification case with performance going from 92.97% to 86.42% of correct identification when switching from the Krawtchouk to the pseudo-Zernike approach. This performance difference is confirmed in the target characterization case with correct target characterization of 84.58% using the Krawtchouk versus the 77.74% obtained with the pseudo-Zernike. The identification and characterization results, with 6.55% and 6.89% of improvements in performance, respectively, confirm the capability of the Krawtchouk moments to represent with higher fidelity smaller details of the targets. Analyzing the performance in the best case (190 brightest scatterers case) of the approach presented in [5] that is reported in Fig. 2(b), it is shown that the brightest-scatterer-based approach provides 96.83%, 93.81%, and 83.67% of correct target recognition,

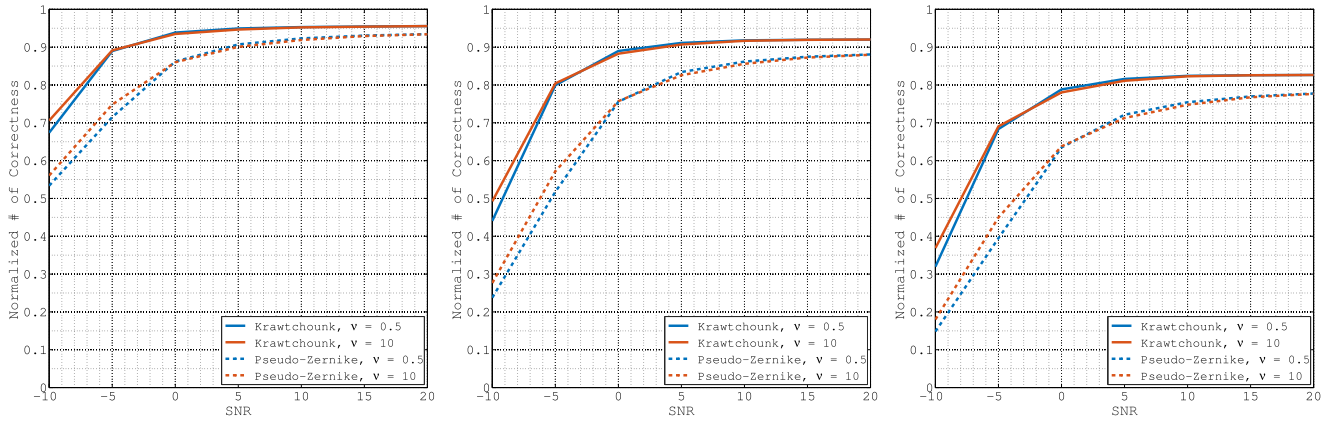

Fig. 3. Performance using Krawtchouck (continuous lines) and pseudo-Zernike (dashed lines) approaches, moments up to order 10, different SNR levels and values of the parameter ν in (10) equal to 0.5 and 10. (a) Recognition. (b) Identification. (c) Characterization.

identification, and characterization, respectively. This performance is comparable with those achievable using the proposed Krawtchouk-based algorithm.

To demonstrate the higher robustness to noise of the Krawtchouk-based approach, a stress analysis under different noise conditions has been performed. In the experiments, additive and multiplicative noise are added to the dataset that are assumed to initially contain noise free images.

A. Additive Compound Gaussian Noise

For each pixel of the image, the additive noise d is modeled as a compound-Gaussian random variable [19], [20], which can be written in the form

$$d = \sqrt{\tau} g \tag{9}$$

where τ is a positive real random variable, and g is a complex circularly symmetric zero-mean Gaussian variable, whose variance is set in order to achieve a certain SNR.

As the variable τ follows a Gamma distribution

$$f(x) = \frac{1}{\Gamma(\nu)} \frac{1}{\mu^{\nu}} x^{\nu-1} e^{-x/\mu} u(x) \tag{10}$$

where $u(\cdot)$ is the unit-step function, μ and ν are the scale and shape parameters, respectively (we set $\mu = 1/\nu$ in order to have a gamma distribution with unit mean). Equations (9) and (10) ensure that the amplitude probability density function of d is K-distributed. SNR levels between -10 and 20 dB and values of ν of 0.5 and 10 are considered. Fig. 3 shows that the results using the Krawtchouk moment approach are more reliable and robust to noise than the pseudo-Zernike one. For example, it is noticed from Fig. 3 that considering an SNR level of 0 dB and $\nu = 0.5$ (impulsive noise), the Krawtchouk moment performance is 93.86%, 88.99%, and 78.83% for recognition, identification, and characterisation, respectively, while using pseudo-Zernike moments, the performance dropped to 86.20%, 75.58%, and 63.48%. In this case, the use of the proposed approach is able to provide more robust results in presence of additional noise in the images, with performance improvement of 7.66% in recognition, 13.41% in identification, and 15.35% in characterization.

The confusion matrices showing the percentage of correct characterization obtained for $\nu = 0.5$ and moments up to order 10 (121 features) are reported in Tables II and III, for Krawtchouk and pseudo-Zernike approaches, respectively. A figure of merit for the overall performance of ATR algorithms considers the ratio of the sum of the values appearing in the diagonal of the confusion matrix to the sum of all the other values. This should have a value as high as possible, which is infinite for a perfect algorithm [21]. In this paper, this figure of merit will be referred to β, which is computed as 3.65 and 1.69 from Tables II and III, respectively.

Moreover, the tables show that in presence of different configurations of the same vehicle (like BMP2 and T72), the capability of target characterization of the Krawtchouk-based algorithm is superior compared to the pseudo-Zernike. For example, considering the two 3×3 top-left matrices of the confusion matrices relative to the BMP2 and T72 targets, and marked in red and blue for clarity, it is seen that both exhibit a more "diagonal" behavior in the Krawtchouk case than in the pseudo-Zernike one. In particular, the figure of merit β is 1.56 and 1.02 when the red matrices are considered and 4.62 and 2.83 for the blue matrices in the Krawtchouk and pseudo-Zernike cases, respectively. These latest results demonstrate the capability of the Krawtchouk moments to maintain a good representation of details in presence of noise.

B. Multiplicative Noise

In the multiplicative noise case, the modulus of each pixel is multiplied with a square root of a Gamma random variable, whose scale and shape parameters are chosen as $\mu = 1/\nu$. Moments of order between 1 and 20 and values of ν of 0.5 and 10 have been considered, and the results obtained in this analysis are shown in Fig. 4. As seen in Fig. 4, in this situation, the performance obtained using

TABLE II
Confusion Matrix Showing the Percentage of Correct Characterization Using Krawtchouk, SNR 0 dB, Order 10, and Additive Compound Gaussian Noise, $\nu = 0.5$

	BMP2 9563	BMP2 9566	BMP2 C21	T72 132	T72 812	T72 S7	2S1	T62	ZSU	BTR70 C71	BTR60	ZIL131	BRDM	D7
BMP2 9563	65.06%	11.38%	18.62%	0.20%	1.00%	0.45%	1.12%	0.27%	0.33%	0.16%	0.06%	0.06%	0.27%	1.00%
BMP2 9566	23.38%	59.69%	11.37%	0.25%	1.08%	1.12%	0.28%	0.42%	0.59%	1.31%	0.21%	0.22%	0.09%	0.00%
BMP2 C21	30.97%	14.91%	48.58%	0.91%	0.92%	0.55%	1.29%	0.29%	0.19%	0.84%	0.02%	0.20%	0.24%	0.12%
T72 132	0.58%	0.53%	1.38%	84.75%	4.20%	5.13%	0.08%	0.54%	2.13%	0.02%	0.04%	0.43%	0.03%	0.17%
T72 812	0.44%	0.69%	0.93%	3.89%	76.90%	13.79%	0.22%	0.97%	1.61%	0.22%	0.03%	0.29%	0.00%	0.02%
T72 S7	0.48%	1.40%	0.79%	9.04%	14.23%	70.76%	0.12%	0.52%	0.91%	0.32%	0.51%	0.80%	0.02%	0.08%
2S1	1.16%	2.08%	2.64%	0.41%	0.84%	0.15%	85.96%	0.28%	0.28%	3.75%	0.48%	0.81%	0.45%	0.71%
T62	2.14%	1.67%	3.00%	2.86%	1.98%	2.04%	2.93%	77.15%	2.90%	0.66%	0.48%	1.01%	0.82%	0.35%
ZSU	1.13%	0.55%	1.37%	1.47%	0.04%	0.20%	0.47%	2.67%	89.03%	0.85%	0.14%	0.02%	0.45%	1.61%
BTR70 C71	0.25%	0.29%	0.74%	0.28%	0.48%	0.06%	0.70%	0.09%	0.01%	92.75%	2.30%	1.00%	1.04%	0.00%
BTR60	0.68%	0.37%	1.53%	0.21%	0.14%	1.14%	0.29%	0.83%	1.09%	3.42%	88.13%	0.49%	1.35%	0.34%
ZIL131	2.15%	0.87%	1.69%	0.95%	0.86%	1.40%	5.08%	0.90%	0.32%	2.59%	0.51%	79.22%	2.90%	0.57%
BRDM	1.31%	2.15%	1.65%	0.84%	0.47%	0.94%	3.17%	1.65%	3.27%	3.39%	1.11%	0.98%	78.13%	0.95%
D7	0.26%	0.54%	0.72%	0.08%	0.00%	0.05%	0.12%	0.08%	0.32%	0.00%	0.32%	0.01%	0.59%	96.91%

TABLE III
Confusion Matrix Showing the Percentage of Correct Characterization Using Pseudo-Zernike, SNR 0 dB, Order 10, and Additive Compound Gaussian Noise, $\nu = 0.5$

	BMP2 9563	BMP2 9566	BMP2 C21	T72 132	T72 812	T72 S7	2S1	T62	ZSU	BTR70 C71	BTR60	ZIL131	BRDM	D7
BMP2 9563	49.06%	15.43%	22.36%	1.54%	0.80%	1.38%	1.91%	0.79%	0.29%	2.60%	0.61%	1.34%	1.53%	0.35%
BMP2 9566	24.53%	42.68%	18.41%	1.82%	1.29%	2.38%	1.78%	0.73%	0.33%	2.90%	0.71%	1.13%	1.20%	0.11%
BMP2 C21	28.45%	18.47%	39.30%	0.99%	1.07%	2.37%	2.24%	1.31%	0.41%	2.06%	0.61%	0.85%	1.20%	0.66%
T72 132	2.85%	3.05%	3.04%	65.09%	6.29%	10.04%	0.79%	2.79%	1.45%	0.51%	1.09%	1.73%	0.53%	0.74%
T72 812	2.57%	2.77%	2.06%	7.25%	55.82%	19.74%	1.36%	2.43%	1.62%	0.79%	1.13%	1.55%	0.20%	0.72%
T72 S7	2.08%	3.46%	2.67%	9.93%	10.66%	60.46%	0.74%	1.68%	1.64%	1.37%	0.94%	2.35%	0.48%	1.54%
2S1	1.90%	5.91%	3.64%	1.30%	1.44%	2.26%	60.06%	2.31%	2.93%	10.78%	0.70%	4.49%	0.83%	1.46%
T62	5.51%	4.55%	8.71%	4.34%	3.29%	4.75%	4.62%	49.85%	2.88%	2.98%	2.30%	1.83%	2.20%	2.20%
ZSU	0.84%	0.89%	1.17%	1.47%	0.39%	0.95%	0.77%	7.06%	77.18%	0.02%	0.61%	0.31%	0.98%	7.35%
BTR70 C71	2.47%	2.36%	2.32%	0.27%	0.11%	0.12%	1.68%	0.70%	0.02%	85.52%	1.16%	0.95%	2.27%	0.05%
BTR60	1.43%	1.96%	2.02%	1.27%	0.36%	1.76%	0.99%	1.59%	0.86%	8.46%	75.01%	1.05%	2.70%	0.54%
ZIL131	1.83%	2.34%	3.76%	2.60%	1.76%	1.36%	6.47%	2.85%	0.58%	6.73%	3.43%	63.84%	1.66%	0.79%
BRDM	1.70%	2.92%	1.23%	0.72%	0.44%	1.04%	3.30%	1.75%	1.94%	4.30%	3.31%	0.85%	74.72%	1.78%
D7	1.84%	0.71%	1.79%	1.16%	0.40%	2.17%	1.45%	2.22%	5.18%	0.15%	0.44%	0.40%	0.70%	81.38%

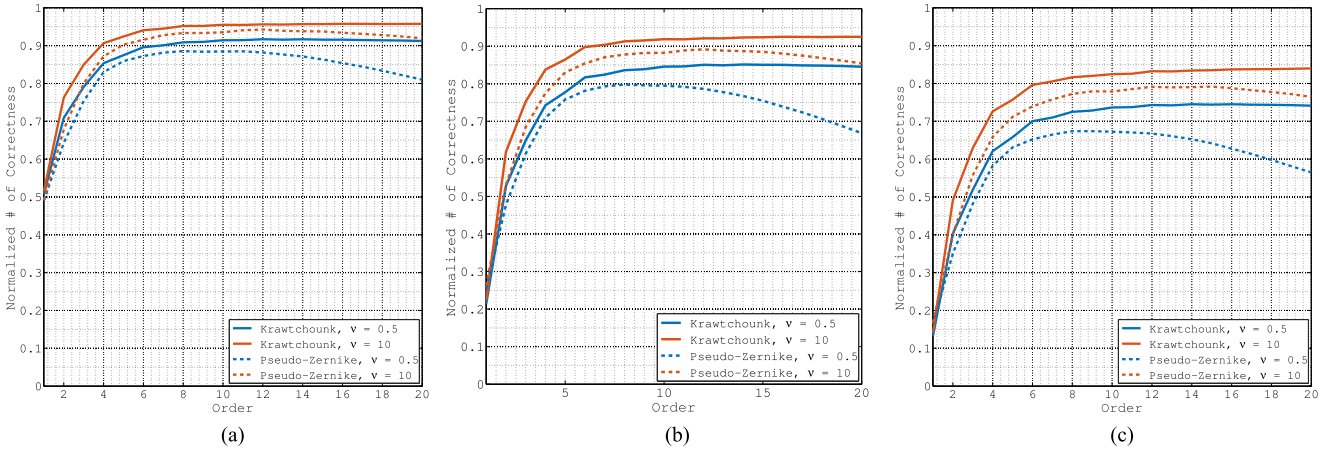

Fig. 4. Performance using Krawtchouck (continuous lines) and pseudo-Zernike (dashed lines) approaches, for different moment orders and multiplicative noise levels with $\nu = 0.5$ and $\nu = 10$. (a) Recognition. (b) Identification. (c) Characterization.

TABLE IV
Confusion Matrix Showing the Percentage of Correct Characterization Using Krawtchouk, Order 10, and Multiplicative Noise, $\nu = 0.5$

	BMP2 9563	BMP2 9566	BMP2 C21	T72 132	T72 812	T72 S7	2S1	T62	ZSU	BTR70 C71	BTR60	ZIL131	BRDM	D7
BMP2 9563	55.57%	14.27%	20.48%	1.07%	1.55%	0.88%	1.79%	0.91%	0.62%	0.33%	0.36%	0.36%	0.60%	1.21%
BMP2 9566	20.85%	55.14%	14.81%	1.09%	1.02%	1.81%	1.40%	0.69%	0.96%	0.79%	0.21%	0.78%	0.38%	0.07%
BMP2 C21	26.77%	17.64%	45.04%	1.15%	0.98%	0.76%	2.33%	1.56%	0.68%	0.57%	0.27%	0.59%	0.73%	0.96%
T72 132	1.15%	1.25%	1.59%	76.36%	5.05%	6.99%	0.33%	1.63%	3.40%	0.06%	0.34%	1.41%	0.06%	0.38%
T72 812	0.48%	0.98%	1.38%	5.35%	69.12%	16.32%	0.42%	2.06%	2.36%	0.17%	0.23%	1.02%	0.03%	0.10%
T72 S7	0.93%	1.51%	1.07%	9.96%	14.58%	64.92%	0.51%	1.02%	2.39%	0.27%	0.30%	1.89%	0.36%	0.30%
2S1	1.79%	2.03%	2.92%	0.57%	0.88%	0.68%	82.40%	1.13%	0.60%	3.34%	0.61%	1.52%	0.30%	1.25%
T62	1.92%	1.37%	2.68%	3.17%	2.98%	3.02%	3.53%	70.35%	5.66%	0.43%	0.89%	1.64%	0.91%	1.46%
ZSU	0.78%	0.56%	1.16%	0.94%	0.16%	0.47%	0.71%	3.06%	87.99%	0.43%	0.36%	0.13%	0.44%	2.80%
BTR70 C71	1.06%	0.74%	0.96%	0.47%	0.88%	0.32%	2.96%	0.52%	0.16%	86.43%	2.95%	1.14%	1.36%	0.04%
BTR60	1.22%	1.07%	1.39%	0.69%	0.34%	1.22%	1.19%	1.68%	1.74%	4.35%	81.33%	1.16%	1.31%	1.31%
ZIL131	1.85%	1.19%	1.75%	1.43%	1.27%	1.50%	6.79%	2.30%	0.74%	2.13%	0.82%	74.85%	1.94%	1.43%
BRDM	2.45%	1.90%	2.40%	0.88%	0.32%	1.20%	5.00%	2.56%	4.12%	2.65%	1.89%	1.05%	72.53%	1.04%
D7	0.40%	0.23%	0.65%	0.08%	0.01%	0.10%	0.30%	0.30%	1.19%	0.01%	0.12%	0.18%	0.43%	96.00%

TABLE V
Confusion Matrix Showing the Percentage of Correct Characterization Using Pseudo-Zernike, Order 10, and Multiplicative Noise, $\nu = 0.5$

	BMP2 9563	BMP2 9566	BMP2 C21	T72 132	T72 812	T72 S7	2S1	T62	ZSU	BTR70 C71	BTR60	ZIL131	BRDM	D7
BMP2 9563	46.98%	17.16%	23.11%	1.76%	0.70%	1.68%	1.88%	0.96%	0.37%	1.89%	0.52%	1.03%	1.42%	0.54%
BMP2 9566	21.53%	44.78%	19.70%	1.67%	1.24%	2.89%	2.00%	0.72%	0.65%	2.32%	0.79%	0.95%	0.63%	0.12%
BMP2 C21	25.81%	18.69%	40.79%	1.59%	1.05%	2.39%	2.58%	1.28%	0.41%	1.46%	0.86%	1.09%	0.99%	1.02%
T72 132	2.25%	2.11%	2.19%	66.52%	5.98%	11.28%	0.80%	2.65%	1.59%	0.22%	1.28%	1.81%	0.18%	1.14%
T72 812	1.06%	1.47%	1.23%	7.49%	56.06%	21.91%	2.28%	3.34%	1.37%	0.35%	0.65%	1.86%	0.12%	0.79%
T72 S7	1.29%	2.16%	1.71%	11.26%	10.10%	61.79%	1.07%	2.33%	1.67%	0.71%	0.89%	3.01%	0.15%	1.85%
2S1	1.67%	3.85%	3.20%	0.97%	1.70%	2.57%	67.12%	3.18%	1.79%	6.58%	0.95%	4.42%	0.48%	1.52%
T62	2.32%	1.51%	4.07%	3.51%	2.94%	5.30%	5.77%	63.20%	4.29%	0.84%	1.44%	1.73%	0.99%	2.09%
ZSU	0.35%	0.49%	0.42%	0.63%	0.18%	0.67%	0.31%	5.65%	83.33%	0.00%	0.26%	0.58%	0.27%	6.86%
BTR70 C71	2.49%	2.55%	2.45%	0.17%	0.24%	0.41%	2.96%	0.80%	0.05%	83.92%	1.86%	0.47%	1.55%	0.08%
BTR60	1.54%	1.46%	1.93%	1.30%	0.62%	2.15%	1.91%	1.81%	1.37%	7.00%	75.61%	0.72%	1.73%	0.86%
ZIL131	0.87%	1.09%	2.16%	1.37%	1.20%	1.46%	7.42%	3.84%	0.82%	2.39%	2.12%	72.70%	0.86%	1.69%
BRDM	1.66%	2.53%	1.59%	0.87%	0.45%	0.89%	2.59%	1.85%	1.56%	3.47%	2.13%	0.69%	77.83%	1.89%
D7	0.58%	0.22%	0.89%	0.40%	0.16%	1.11%	0.76%	2.10%	6.02%	0.01%	0.24%	0.81%	0.33%	86.38%

the Krawtchouk approach results in higher reliability and robustness to noise compared to those obtained using the pseudo-Zernike. For example, considering an SNR level of 0 dB and $\nu = 0.5$, the algorithm using the Krawtchouk moments results to be correct in 91.43%, 84.57%, and 73.65% of cases for recognition, identification, and characterisation, respectively, while using the pseudo-Zernike moments, the performance dropped to 88.46%, 79.50%, and 67.25%. In this case, the use of the proposed approach is able to provide more robust results in the presence of multiplicative noise in the images, with performance improvement of 2.97% in recognition, 5.07% in identification, and 6.40% in characterization capabilities. For completeness, the confusion matrices showing the percentage of correct characterization obtained for the $\nu = 0.5$ and moments up to order 10 are reported in Tables IV and V for Krawtchouk and pseudo-Zernike, respectively. In these cases, β results to have the values of 2.66 and 1.96, respectively. Again, in red and blue, the variations of BMP2 and T72 are reported. Also, for the multiplicative noise case, the Krawtchouk moments show a better capability to maintain a good representation of details compared to those obtained using the pseudo-Zernike moments; in particular, β results to be 1.35 and 1.05 for the BMP2 target and 3.61 and 2.71 for the T72 case for the Krawtchouk and pseudo-Zernike approaches, respectively.

These results demonstrate the higher robustness to the presence of noise of the Krawtchouk moments, making the proposed approach particularly suitable for more noisy SAR images like those acquired with low-cost sensors mounted on UAVs and low-frequency SAR images (e.g., foliage-penetrating SAR).

IV. CONCLUSION

In this paper, an algorithm for ATR based on the Krawtchouk moments has been presented. The proposed approach was shown to provide a more reliable solution to the ATR challenge from SAR images with higher capabilities in discriminating between different subclasses of targets and in noisy environments. The performance of the proposed algorithm was assessed using the real MSTAR

dataset that contains different vehicles in various configurations. The superior performance and robustness of the Krawtchouk-based algorithm have been confirmed by the experimental results, demonstrating improvements, in particular, on the characterization of targets, over the approach using the pseudo-Zernike moments that suffers from discretization errors and is less robust in the presence of noise. Hence, the proposed approach is particularly suitable for SWAP systems and with potential to be used on SAR images acquired with low-cost sensors mounted on UAVs and foliage-penetrating SAR images.

CARMINE CLEMENTE, *Member, IEEE*
University of Strathclyde, Glasgow, U.K.

LUCA PALLOTTA, *Member, IEEE*
CNIT c/o Università di Napoli, Napoli, Italy

DOMENICO GAGLIONE, *Student Member, IEEE*
University of Strathclyde, Glasgow, U.K.

ANTONIO DE MAIO, Fellow, IEEE
Università di Napoli "Federico II", Napoli, Italy

JOHN J. SORAGHAN, *Senior Member, IEEE*
University of Strathclyde, Glasgow, U.K.

REFERENCES

[1] L. M. Novak, S. D. Halversen, G. J. Owirka, and M. Hiett
Effects of polarization and resolution on SAR ATR
IEEE Trans. Aerosp. Electron. Syst., vol. 33, no. 1, pp. 102–116, Jan. 1997.

[2] L. Novak, G. Owirka, and A. Weaver
Automatic target recognition using enhanced resolution SAR data
IEEE Trans. Aerosp. Electron. Syst., vol. 35, no. 1, pp. 157–175, Jan. 1999.

[3] C. Clemente, M. Di Bisceglie, M. Di Santo, N. Ranaldo, and M. Spinelli
Processing of synthetic aperture radar data with GPGPU
In *Proc. IEEE Workshop Signal Process. Syst.*, Oct. 2009, pp. 309–314.

[4] Z. Qun and J. Principe
Support vector machines for SAR automatic target recognition
IEEE Trans. Aerosp. Electron. Syst., vol. 37, no. 2, pp. 643–654, Apr. 2001.

[5] S. H. Doo, G. Smith, and C. Baker
Reliable target feature extraction and classification using potential target information
In *Proc. IEEE Radar Conf.*, May 2015, pp. 628–633.

[6] U. Srinivas, V. Monga, and R. Raj
SAR automatic target recognition using discriminative graphical models
IEEE Trans. Aerosp. Electron. Syst., vol. 50, no. 1, pp. 591–606, Jan. 2014.

[7] M. Krawtchouk
On interpolation by means of orthogonal polynomials
Memoirs Agricultural Inst. Kyiv, vol. 4, pp. 21–28, 1929.

[8] P.-T. Yap, R. Paramesran, and S.-H. Ong
Image analysis by Krawtchouk moments
IEEE Trans. Image Process., vol. 12, no. 11, pp. 1367–1377, Nov. 2003.

[9] W. A. Jassim, R. Paramesran, and M. S. A. Zilany
Enhancing noisy speech signals using orthogonal moments
IET Signal Process., vol. 8, no. 8, pp. 891–905, 2014.

[10] P. A. Raj
A Krawtchouk moments based super resolution technique for multiframe image sequence
In *Proc. IEEE 16th Int. Symp. Consum. Electron.*, Jun. 2012, pp. 1–3.

[11] D. Ioannidis, D. Tzovaras, I. G. Damousis, S. Argyropoulos, and K. Moustakas
Gait recognition using compact feature extraction transforms and depth information
IEEE Trans. Inf. Forensics Security, vol. 2, no. 3, pp. 623–630, Sep. 2007.

[12] A. Mademlis, A. Axenopoulos, P. Daras, D. Tzovaras, and M. G. Strintzis
3D content-based search based on 3D krawtchouk moments
In *Proc. 3rd Int. Symp. 3D Data Process., Vis., Transmiss.*, Jun. 2006, pp. 743–749.

[13] M. Teague
Image analysis via the general theory of moments
J. Opt. Soc. Amer., vol. 70, no. 8, pp. 920–930, 1980.

[14] C. H. Teh and R. Chin
On image analysis by the methods of moments
IEEE Trans. Pattern Anal. Mach. Intell., vol. 10, no. 4, pp. 496–513, Jul. 1988.

[15] K. Fukunaga
Introduction to Statistical Pattern Recognition (ser. Computer Science and Scientific Computing). Amsterdam, The Netherlands: Elsevier Science, 1990.

[16] T. Ross, S. Worrell, V. Velten, J. Mossing, and M. Bryant
Standard SAR ATR evaluation experiments using the MSTAR public release data set
Proc. SPIE, vol. 3370, pp. 566–573, 1998.

[17] MSTAR image database, 1997. [Online]. Available: https://www.sdms.afrl.af.mil/index.php?collection=mstar. Accessed on: Oct. 2016.

[18] C. Clemente, L. Pallotta, I. Proudler, A. De Maio, J. Soraghan, and A. Farina
Pseudo-Zernike based multi-pass automatic target recognition from multi-channel synthetic aperture radar
IET Radar, Sonar Navigat., vol. 9, no. 4, pp. 457–466, 2015.

[19] E. Conte and M. Longo
Characterisation of radar clutter as a spherically invariant random process
IEE Proc. Commun., Radar Signal Process., vol. 134, no. 2, pp. 191–197, Apr. 1987.

[20] M. Greco and F. Gini
Statistical analysis of high-resolution SAR ground clutter data
IEEE Trans. Geosci. Remote Sens., vol. 45, no. 3, pp. 566–575, Mar. 2007.

[21] P. Tait
Introduction to Radar Target Recognition (ser. IEE Radar Series). Stevenage, U.K.: Inst. Eng. Technol., 2005.